

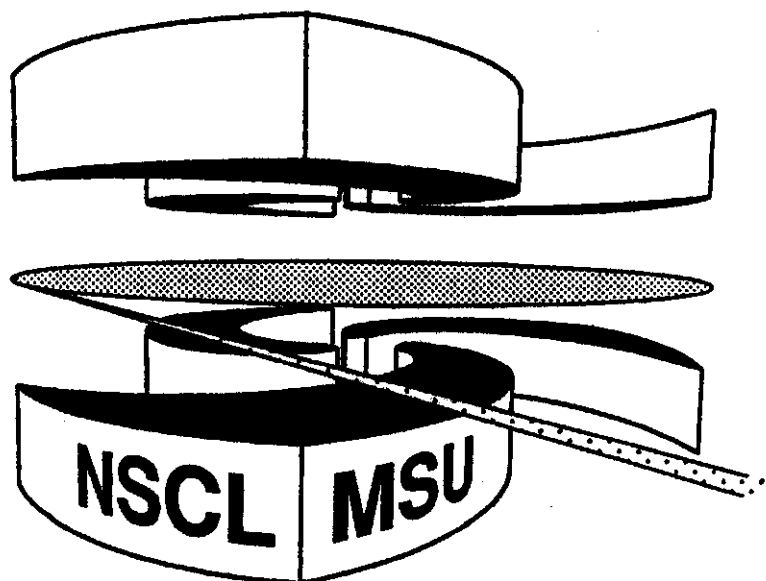


Michigan State University

National Superconducting Cyclotron Laboratory

**HIGHER EXCITATIONS OF  $\omega$  AND  $\phi$  IN DILEPTON SPECTRA**

**KEVIN HAGLIN and CHARLES GALE**



## Higher excitations of $\omega$ and $\phi$ in dilepton spectra

Kevin Haglin\*

National Superconducting Cyclotron *Laboratory*, Michigan State University  
East Lansing, Michigan 48824-1321

Charles Gale†

Physics Department, *McGill* University, 3600 University St., *Montréal, Québec, H3A 2T8*,  
Canada

(October 11, 1994)

### Abstract

We consider lepton pair production via two-hadron annihilation through various isoscalar vector mesons within hot, baryon-free matter. This is tantamount to constructing effective form factors which we model using a vector-meson-dominance approach and compare with experiment. In particular, we consider the reactions  $\pi\rho \rightarrow e^+e^-$  and  $\bar{K}K^*(892) + \text{c.c.} \rightarrow e^+e^-$ . We find that  $\omega(1390)$  and  $\phi(1680)$  are visible in the mass spectrum for the thermal production rate above the  $\pi^+\pi^- \rightarrow e^+e^-$  tail and even above the  $\pi a_1 \rightarrow e^+e^-$  results-both of which were considered dominant in their respective mass regions.

PACS numbers: 25.75.+r, 12.38.Mh, 13.75.Lb

## I. INTRODUCTION

Production of dileptons in high-energy heavy-ion collisions continues to be studied actively since it is hoped that such signals might be useful in discriminating prehadronic or quantum chromodynamic (QCD) plasma formation from ordinary hadronic matter. The possible success depends on having a reasonably complete picture of both plasma and hadronic phases. Crossover from one to the other is expected for a critical temperature in the neighborhood of 200 MeV and near this boundary the hadronic matter will be populated by many species of strange and nonstrange mesons. However, to get a rough idea about this phase of matter one typically uses a simple pion-gas approximation. In terms of dilepton spectra, it has recently been shown that thermal dielectron production rates from the pion gas were an order of magnitude lower than what the authors were calling the total hadronic rate [1]. Going beyond pion gas considerations is important. Allowing heavier species to partially comprise the system complicates matters since each species might interact among themselves as well as with others. The list of possible processes then becomes quite lengthy. Further complications or uncertainties arise since, with the exception of the pion [2], hadronic form factors are not particularly well known. Reactions which involve an intermediate isoscalar vector meson could contribute to dilepton production and for this reason the mass distribution of produced dileptons is expected to exhibit structure owing to these hadronic resonances.

Observed spectra from heavy-ion collisions will of course be restricted to a time-integrated yield. Temperature (or time) dependent rates are the essential quantity that might be input for models of the time evolution in order to make predictions for overall yields. Rate calculations have been done with various levels of sophistication. In a quest for more accurate knowledge of dielectron production rates we consider some hadronic processes which produce  $e^+e^-$  pairs and then compare with spectra calculated previously [1,3]. The particular processes we consider are pseudoscalar and vector reactions of the type  $P + V \rightarrow V^{I=0} \rightarrow e^+e^-$  where  $P$  and  $V$  are either pions and  $\rho$ -mesons or kaons and  $K^*$ s. The intermediate isoscalar vector hadronic resonances are  $\phi(1020)$ ,  $\omega(1390)$  and  $\omega(1600)$  for the  $\pi\rho$  processes and  $\phi(1680)$  for the strange-particle process. Special attention is paid to experimental data on the time-reversed processes in order to constrain or even fix the coupling constants.

Our paper is organized in the following way. In Sect. II we present the basic formalism for the interactions among the hadronic degrees of freedom and the elementary scattering (annihilation) processes. A vector-meson-dominance (VDM) approach will be presented which allows calculation of the basic Feynman diagram for  $a+b \rightarrow V^{I=0} \rightarrow \gamma^* \rightarrow e^+e^-$ . Within this approach the amplitude for each diagram contains a ratio of the strong-to-electromagnetic coupling constants. Experimental data on cross sections for the time reversed processes  $e^+e^- \rightarrow a+b$  are shown as compared with model calculations. These are used to fix coupling constants and phases between diagrams. One is really constructing an effective form factor by this prescription. Section III contains the essential details and results for thermal production rates which include effects from these hadronic resonances. The interesting result is that the  $\omega(1390)$  and  $\phi(1680)$  peaks are visible above the rate from  $\pi^+\pi^-$  annihilation and even  $\pi a_1$  reactions which have recently been shown to be dominant for restricted masses [3]. Finally, in Sect. IV we conclude with some final remarks which essentially stress the importance of appealing to experimental data at some level for the elementary reactions in

future studies. Putting them into calculations on systems of hadronic matter only after such comparison minimizes uncertainty.

## II. FORMALISM

After the initial stage of a collision of the type we consider, which may well include a prehadronic or quark-gluon-plasma (QGP) phase, hadronization gives rise to a hot ensemble of low-lying mesons. Within the context of a thermodynamic model this system's composition has recently been studied [4]. The most abundant hadronic species in this scenario are pions, kaons,  $\rho$ -mesons and  $K^*(892)$  strange vector mesons owing to the large spin-isospin degeneracy of the last two. With temperatures ranging from phase boundary or crossover temperature downward toward the pion mass or lower, where the system ceases interacting, the number densities of these species range from several hundredths to a few tenths per  $\text{fm}^3$  [4]. Until freezeout, they interact very strongly. Though binary reactions dominate at these densities, studies of the effect of ternary reactions have been pursued [5].

Species can be classified according to their quantum numbers in order to identify the manner with which we model their interactions. Pseudoscalar particles (P) interact with a vector particle (V) in a manner described by the Lagrangian [6]

$$L_{VPP} = g_{VPP} V^\mu P \overleftrightarrow{\partial}_\mu P \quad (2.1)$$

and vectors interact with a pseudoscalar through

$$L_{VVP} = g_{VVP} \epsilon_{\mu\nu\alpha\beta} \partial^\mu V^\nu \partial^\alpha V^\beta P. \quad (2.2)$$

Let two hadrons, call them  $a$  and  $b$ , scatter in a timelike fashion, i.e. let them annihilate and form an intermediate (virtual) state  $V$ . This state is a vector meson in our study. It is not entirely clear how it converts itself from a hadronic to an electromagnetic field, but we model the phenomenon using the principle of vector-meson dominance. In practice, it means that the neutral component of the hadronic vector field couples directly to the photon via [7]

$$L_{VA} = e \left( \frac{g_{Vab}}{g_V} \right) m_V^2 V^{(3)} \cdot A \quad (2.3)$$

where  $V$  is the resonant vector field and  $A$  is the electromagnetic field. Using Eqs. (2.1) or (2.2) and (2.3) we construct the general annihilation diagram through a vector resonance  $V$  to a virtual or massive photon, which subsequently decays into a lepton pair as shown in Fig 1. This differs from an analogous process of purely electromagnetic exchange because of the presence of the hadronic resonance. Since the effect of this resonance appears as a function of invariant mass alone, the hadronic dependence of  $V$  at the vertex factorizes from the rest of the diagram in Fig. 1 as a form factor times a pointlike electromagnetic process. Vector-meson dominance has been very successful in the areas of hadronic form factors, photoproduction and absorption cross sections, and in the vector meson exchange contributions to  $\pi N$  and  $NN$  scattering.

The presence of the ratio  $g_{Vab}/g_V$  in Eq. (2.3) translates into the same ratio appearing (squared) in the cross section. We will discuss two methods for fixing these quantities. For the case of the  $\phi(1020)$  we can fix these coupling constants independently via strong and electromagnetic decays; whereas for the higher excitations presently considered we are forced to use another procedure. First consider the decay  $\phi \rightarrow \rho\pi$ . We calculate its rate to be

$$\Gamma_{\phi \rightarrow \rho\pi} = \frac{g_{\phi\rho\pi}^2 |\mathbf{p}|^3}{12\pi} \quad (2.4)$$

where  $\mathbf{p}$  is the center-of-mass momentum of the decay products. This determines  $m_\phi^2 g_{\phi\rho\pi}^2 / 4\pi = 0.29$  when the partial decay rate is taken to be 12.9% of 4.43 MeV. The same expression and numerical conclusions were reached in a recent study of  $\phi$ -meson properties at zero and finite temperature [8]. Next, the electromagnetic decay  $\phi \rightarrow e^+e^-$  is modelled and computed to be

$$\Gamma_{\phi \rightarrow e^+e^-} = \frac{e^4 m_\phi}{12\pi g_\phi^2}. \quad (2.5)$$

Using the branching fraction  $\Gamma_{\phi \rightarrow e^+e^-} / \Gamma_\phi^{\text{full}} = 3.09 \times 10^{-4}$ , we arrive at the dimensionless vector-dominance coupling constant for the  $\phi$  of  $g_\phi = 12.9$ .

Since data are not sufficient to allow us to follow this prescription for the other resonances, we instead appeal to the time-reversed hadron production processes

$$e^+e^- \rightarrow a + b + \dots \quad (2.6)$$

We compute the cross sections for  $e^+e^- \rightarrow \rho\pi$  and for  $e^+e^- \rightarrow \bar{K}K^*(892)$  which is approximated by  $e^+e^- \rightarrow K_S^0 K^\pm \pi^\mp$ . The diagrams are shown in Figs. 2 a and b. The cross section for the process in Fig. 2a is found to be

$$\sigma_{e^+e^- \rightarrow \rho\pi}(M) = \frac{e^4 |\mathbf{p}|^3 |F_{\pi\rho}(M)|^2}{12\pi M^3} \quad (2.7)$$

where

$$F_{\pi\rho}(M) = \sum_V \left( \frac{g_{V\pi\rho}}{g_V} \right) \frac{e^{i\varphi_V} m_V^2}{m_V^2 - M^2 - im_V \Gamma_V}, \quad (2.8)$$

with the sum running over the three vectors  $\phi(1020)$ ,  $\omega(1390)$  and  $\omega(1600)$ . Eq. (2.8) is somewhat phenomenological since it contains arbitrary phases between the diagrams. However, comparison with experiment constrains the ratios of coupling constants as well as these phase angles. The comparison to data is shown in Fig. 3. Details of the parameters in our model go as follows. For the phases we take  $\varphi_\phi = 0$  (without loss of generality one of them can be set to zero),  $\varphi_\omega = 5\pi/4$  and  $\varphi_{\omega'} = \pi$ ; while the ratios are taken to be  $g_{\omega\pi\rho}/g_\omega = 0.29 \text{ GeV}^{-1}$  and  $g_{\omega'\pi\rho}/g_{\omega'} = 0.05 \text{ GeV}^{-1}$ . Note that  $g_{\phi\pi\rho}/g_\phi = 0.15 \text{ GeV}^{-1}$  was already fixed by Eqs (2.4–2.5). Notation used here is that  $\phi$  means  $\phi(1020)$ ,  $\omega$  stands for  $\omega(1390)$  and  $\omega'$  is  $\omega(1600)$ .

The amplitude for the strange particle process  $e^+e^- \rightarrow K_S^0 K^\pm \pi^\mp$  as shown in Fig. 2b contains a coupling of the  $K^*$  to  $K\pi$ . This can be fixed by the decay  $K^* \rightarrow K\pi$  which is known experimentally to be  $\sim 50 \text{ MeV}$  and can be computed within our modelling to be

$$\Gamma_{K^* \rightarrow K\pi} = \left( \frac{g_{K^*K\pi}^2}{4\pi} \right) \frac{|\mathbf{p}|}{6m_{K^*}^2} \left\{ \frac{(m_K^2 - m_\pi^2)^2}{m_{K^*}^2} + m_{K^*}^2 - 2m_\pi^2 - 2m_K^2 \right\}. \quad (2.9)$$

The coupling constant is fixed to be  $g_{K^*K\pi}^2/4\pi = 2.47$ . Returning to the full process depicted in Fig. 2b a different form factor is needed

$$F_{KK^*}(M) = \left( \frac{g_{\phi'KK^*}}{g_{\phi'}} \right) \frac{m_{\phi'}^2}{m_{\phi'}^2 - M^2 - im_{\phi'}\Gamma_{\phi'}}, \quad (2.10)$$

where  $\phi'$  is shorthand for  $\phi(1680)$ . The cross section for the full process cannot be written quite so conveniently since it contains a three-body final state. Using massless leptons the differential form looks like

$$d\sigma = \frac{|\mathcal{M}|^2}{2s} (2\pi)^4 \delta^4(p_+ + p_- - p_{K_1} - p_{K_2} - p_\pi) \frac{d^3p_{K_1}}{(2\pi)^3 2E_{K_1}} \frac{d^3p_{K_2}}{(2\pi)^3 2E_{K_2}} \frac{d^3p_\pi}{(2\pi)^3 2E_\pi} \quad (2.11)$$

where the squared amplitude (initial spin averaged and final spin summed) is

$$\begin{aligned} |\mathcal{M}|^2 &= e^4 g_{K^*K\pi}^2 |F_{KK^*}(M)|^2 \frac{1}{M^4} \epsilon_{\mu\nu\alpha\beta} \epsilon_{\kappa\lambda\sigma\tau} q^\mu q^\kappa (p_K + p_\pi)^\alpha (p_K + p_\pi)^\sigma \\ &\times \left( g^{\beta\xi} - (p_K + p_\pi)^\beta (p_K + p_\pi)^\xi / m_{K^*}^2 \right) \left( g^{\tau\zeta} - (p_K + p_\pi)^\tau (p_K + p_\pi)^\zeta / m_{K^*}^2 \right) \\ &\times (p_K - p_\pi)^\xi (p_K - p_\pi)^\zeta L^{\nu\lambda} \left| \frac{1}{(p_K + p_\pi)^2 - m_{K^*}^2 - im_{K^*}\Gamma_{K^*}} \right|^2 \end{aligned} \quad (2.12)$$

where  $p_K$  always refers to the momentum of the kaon which decays from the  $K^*$ ,  $q = p_+ + p_-$  and the leptonic tensor is

$$L^{\nu\lambda} = p_+^\nu p_-^\lambda + p_-^\nu p_+^\lambda - g^{\nu\lambda} (p_+ \cdot p_-). \quad (2.13)$$

Although Eq. (2.12) looks rather complicated, notice that all the  $p^\mu p^\nu / m_{K^*}^2$  terms will vanish since any two identical indices in the Levi-Civita symbol results in zero. After performing the four-vector algebra and after integrating over three-body phase space we arrive at the result presented in Fig. 4. The precise value of the ratio we use to generate this curve is  $g_{\phi'KK^*}/g_{\phi'} = 0.19 \text{ GeV}^{-1}$ .

### III. THERMAL PRODUCTION RATES

Hadrons in this hot reaction zone are assumed to have their momenta thermally distributed. Then the differential rate at which they scatter, i.e. the differential rate at which hadrons annihilate to create an  $e^+e^-$  pair of invariant mass  $M$  can be written as

$$\begin{aligned} \frac{dR}{dM^2} &= \mathcal{N} \int \frac{d^3p_a}{2E_a(2\pi)^3} \frac{d^3p_b}{2E_b(2\pi)^3} \frac{d^3p_+}{2E_+(2\pi)^3} \frac{d^3p_-}{2E_-(2\pi)^3} f(E_a) f(E_b) \\ &\times (2\pi)^4 |\mathcal{M}|^2 \delta^4(p_a + p_b - p_+ - p_-) \delta(M^2 - (p_+ + p_-)^2) \end{aligned} \quad (3.1)$$

where  $f$  is the Bose-Einstein distribution and  $\mathcal{N}$  is an overall degeneracy factor. With the aid of the  $\delta$  functions some of the phase space can be reduced analytically. We integrate the rest numerically.

The absolute square of the scattering amplitude for  $\pi\rho \rightarrow e^+e^-$  (again, initial spin averaged and final spin summed) is

$$|\mathcal{M}|^2 = \frac{4e^4}{3} \frac{|F_{\pi\rho}(M)|^2}{M^4} \epsilon_{\mu\nu\alpha\beta} \epsilon_{\kappa\lambda\sigma\tau} q^\mu q^\kappa p_\rho^\alpha p_\rho^\sigma (g^{\beta\tau} - p_\rho^\beta p_\rho^\tau / m_\rho^2) L^{\nu\lambda} \quad (3.2)$$

where the leptonic tensor of Eq. (2.13) is used and where  $q^\mu = p_+^\mu + p_-^\mu$  so that  $q^2 = M^2$  and finally, where the form factor is given by Eq. (2.8). Making the replacements  $m_\rho \rightarrow m_{K^*}$  and  $p_\rho \rightarrow p_{K^*}$  and using the form factor of Eq. (2.10) instead of Eq. (2.8) gives the squared amplitude for the process  $\bar{K}K^* + \text{c.c.} \rightarrow e^+e^-$ .

After contracting the indices in Eq. (3.2) and performing the thermally weighted phase space integral in Eq. (3.1), we reach the results at 150 MeV temperature presented in Fig. 5. For comparison purposes we also include the results for  $\pi^+\pi^-$  annihilation [1] and for  $\pi a_1$  reactions Ref. [3] which were concluded to be dominant for masses above  $m_\phi$ . The importance of the excitations of  $\omega(1390)$  and  $\phi(1680)$  are immediate: they are visible above the tail of the  $\pi^+\pi^-$  annihilation and even above the  $\pi a_1$  results. One last figure is shown (Fig. 6) where a temperature of 200 MeV is used. Our conclusions are independent of the temperature.

#### IV. FINAL REMARKS

Timelike photons are observed to have a strong affinity for neutral hadronic fields. This observation is captured in the current field identity [12] which is a consequence of the VMD hypothesis. These photons, observed as lepton pairs, exhibit resonant structure when the observed particles are projected onto a mass spectrum. One understands these peaks within vector-meson dominance to be manifestations of hadronic form factors. Our study suggests that in order to improve knowledge of dielectron production rates from hot hadronic matter, at least for dielectron masses ranging from  $m_\phi$  to  $m_{J/\psi}$ , form factors for hadrons other than just the pion must be considered. We show only two examples of additional structure in the mass spectrum—there may well be more surprises.

World data on electron-positron annihilation into hadrons is quite extensive at higher energies but is unfortunately not as complete for lower energies. However, that which does exist should be exploited to its fullest potential. In our study we have constructed effective form factors  $|F_{\pi\rho}(M)|^2$  and  $|F_{KK^*}(M)|^2$  in the mass range 1–2.5 GeV. After doing so, we have compared each elementary process with known data before using them in a thermal calculation on the extended system of interacting hadrons. Higher excitations of the  $\omega$  and  $\phi$ , namely  $\omega(1390)$  and  $\phi(1680)$ , were found to be visible in the mass distribution of the dilepton production rate above the hadronic production mechanisms previously considered.

#### ACKNOWLEDGEMENTS

K.H. acknowledges support from the National Science Foundation under grant number PHY-9403666 and wishes to thank the Physics Department at McGill University for hospitality during a visit in May 1994 when initial stages of this work were discussed. C.G. acknowledges support from the Natural Sciences and Engineering Research Council of Canada, the FCAR of the Québec Government and a NATO Collaborative Research Grant.

## REFERENCES

\* electronic address: haglin@theo03.nscl.msu.edu

† electronic address: gale@prism.physics.mcgill.ca

- [1] C. Gale and P. Lichard, Phys. Rev. D **49**, 3338 (1994).
- [2] DM2 Collaboration, Phys. Lett. **B 220**, 321 (1989).
- [3] C. Song, C. M. Ko and C. Gale, Phys. Rev. D, in press.
- [4] K. Haglin and S. Pratt, Phys. Lett. **B**, in press.
- [5] P. Lichard, University of Minnesota and Theoretical Physics Institute Preprint Number TPI-UMN 92/51-T, October 1992.
- [6] U.-G. Meissner, Phys. Rep. **161**, 213 (1988).
- [7] J. J. Sakurai, Ann. Phys. (N.Y.) **11**, 1 (1960).
- [8] K. Haglin and C. Gale, Nucl. Phys. **B**, in press.
- [9] V. M. Aulchenko *et al.* Novosibirsk Preprint 86-106 (1986); A. Donnachie and A. B. Clegg, Z. Phys. C **42**, 663 (1989).
- [10] R. Baldini-Ferrolì in Proc. Had. Phys. at Intermediate Energy, T. Bressani, B. Menetti, and G. Pauli (eds.) Amsterdam, New York, Elsevier (1987); A. Donnachie and A. B. Clegg, Z. Phys. C **42**, 663 (1989).
- [11] F. Mane, *et al.*, Phys. Lett. **B 112**, 179 (1982).
- [12] N. Kroll, T. D. Lee and B. Zumino, Phys. Rev. **157**, 1376 (1967).



## FIGURES

FIG. 1. General annihilation diagram of two hadrons  $a$  and  $b$  to a lepton pair. The process goes through a vector hadronic resonance  $R$  and by vector-meson dominance, goes directly to a virtual photon.

FIG. 2. Annihilation of  $e^+e^-$  into  $\pi\rho$  through any of three isoscalar vector  $\phi(1020)$ ,  $\omega(1390)$  and  $\omega(1600)$  in (a) and in (b)  $e^+e^- \rightarrow K_S^0 K^\pm \pi^\mp$ .

FIG. 3. Cross section for  $e^+e^- \rightarrow \pi\rho$  as computed within the model described in the text as compared with experimental data from Ref. [9,10].

FIG. 4. Cross section for  $e^+e^- \rightarrow K_S^0 K^\pm \pi^\mp$  again computed with the model described in the text as compared with experimental data from Ref. [11].

FIG. 5. Thermal production rate at  $T = 150$  MeV from  $\pi\rho$  (solid curve) processes,  $\bar{K}K^* + c.c.$  (dotted curve),  $p i^+ \pi^-$  annihilation from Ref. [1] (dot-dash curve) and finally,  $\pi a_1$  process as calculated in Ref. [3] (dashed curve).

FIG. 6. Same as Fig. 5 except using  $T = 200$  MeV.

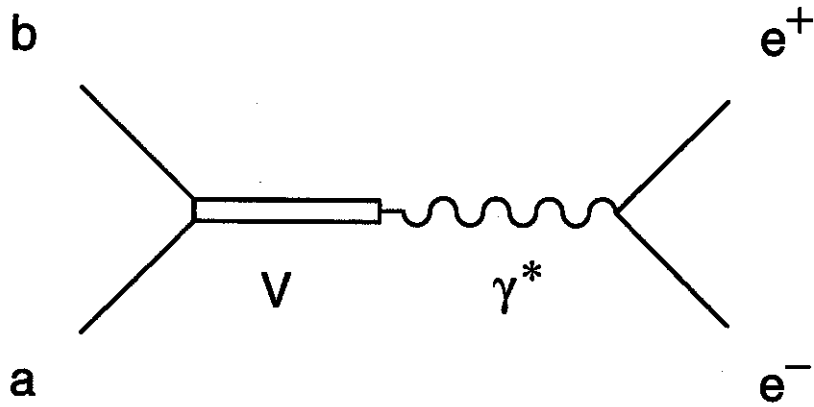


Figure 1

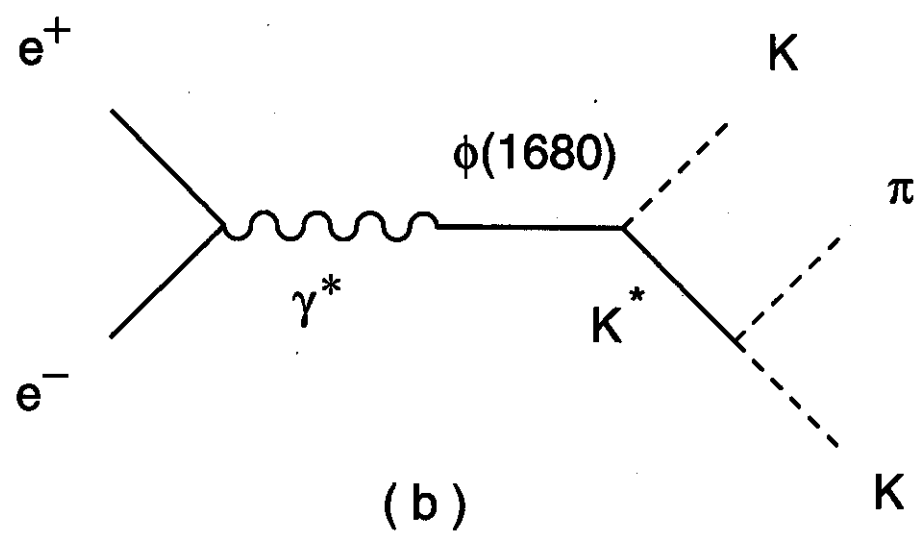
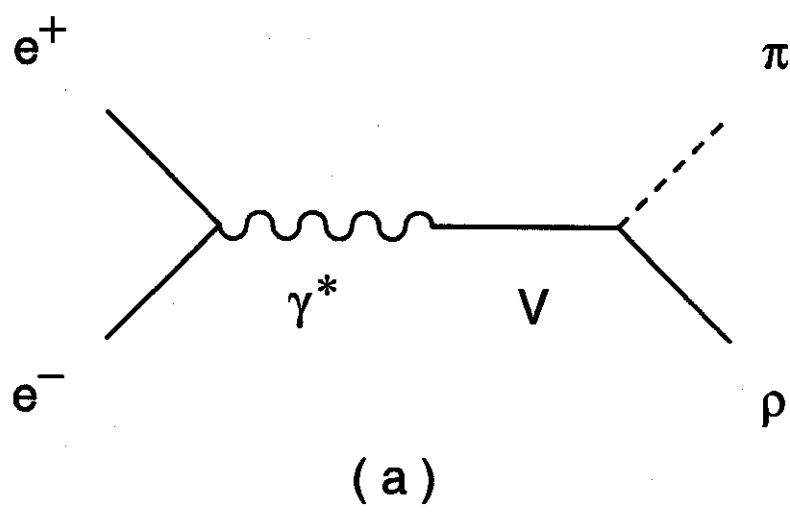
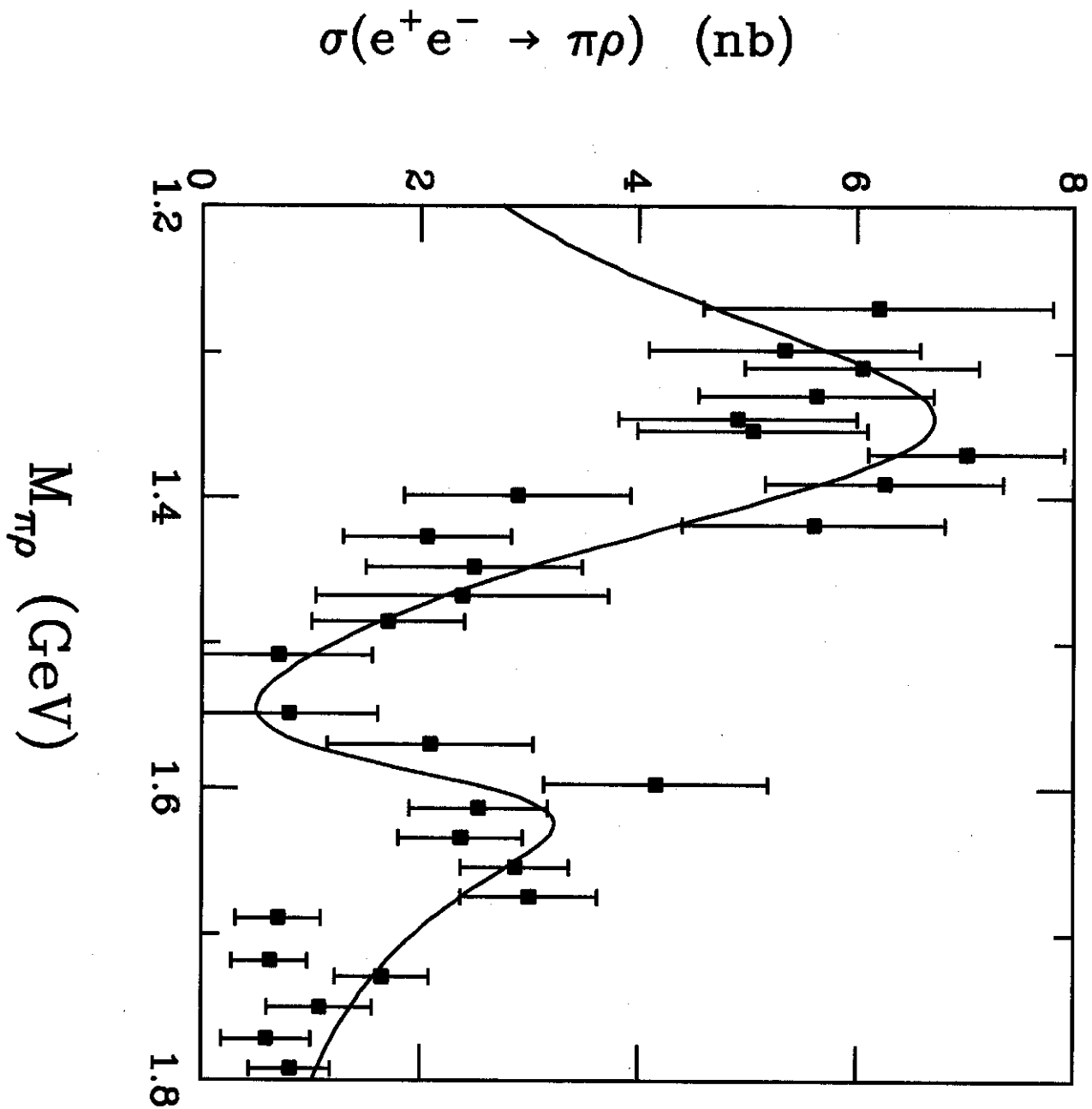


Figure 2

Figure 3



$$\sigma(e^+e^- \rightarrow K_S^0 K^\pm \pi^\mp) \text{ (nb)}$$

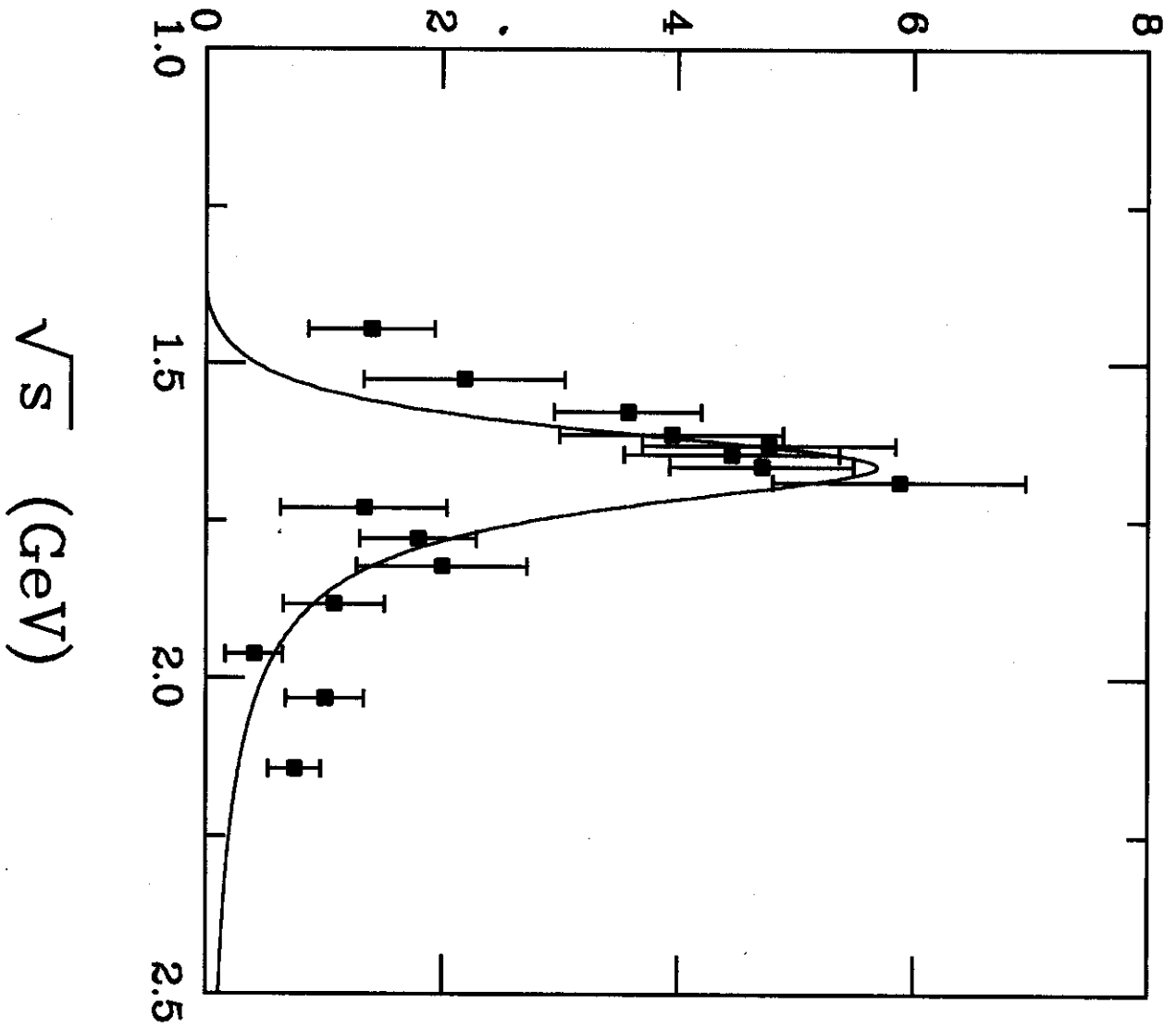


Figure 4

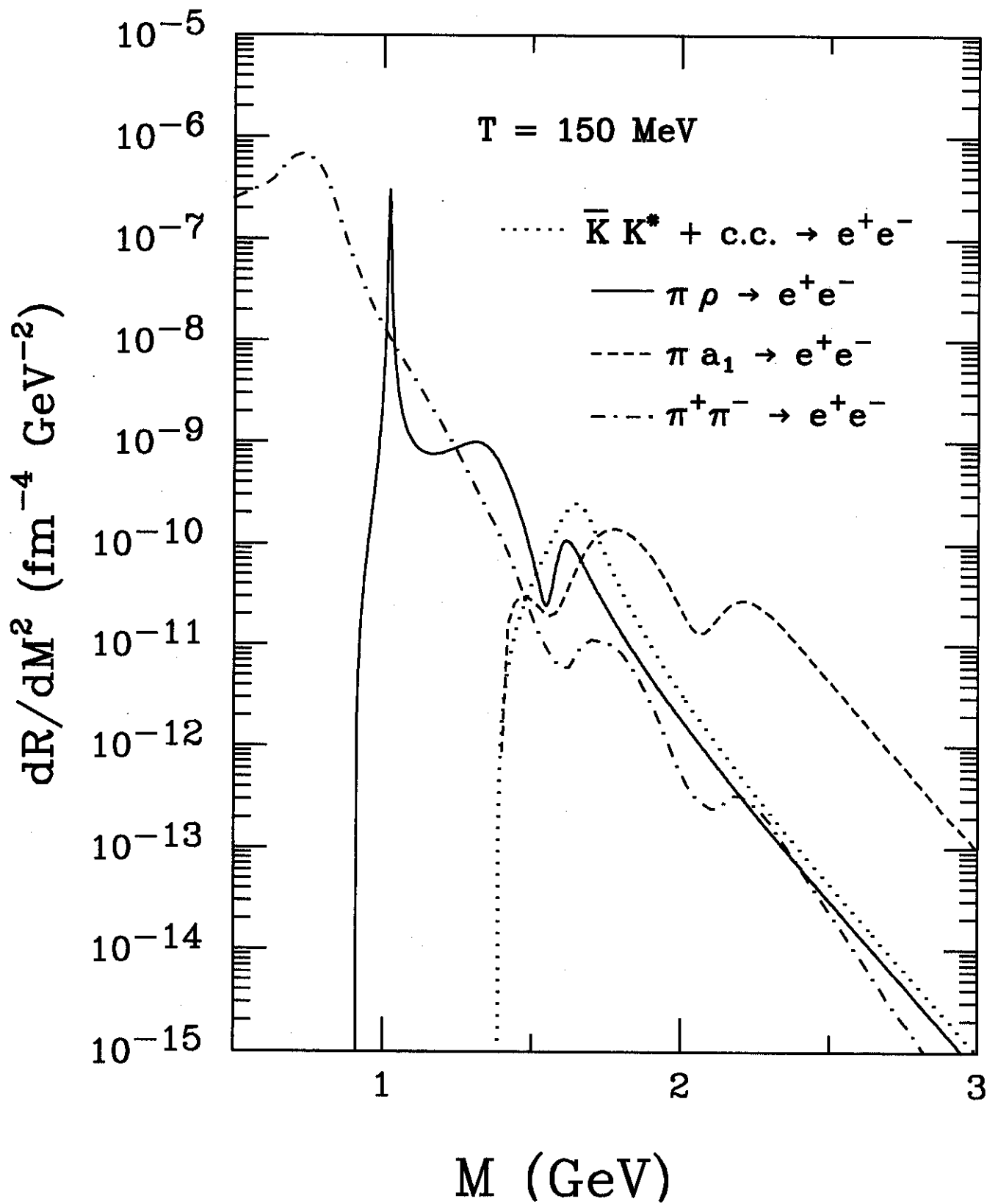


Figure 5

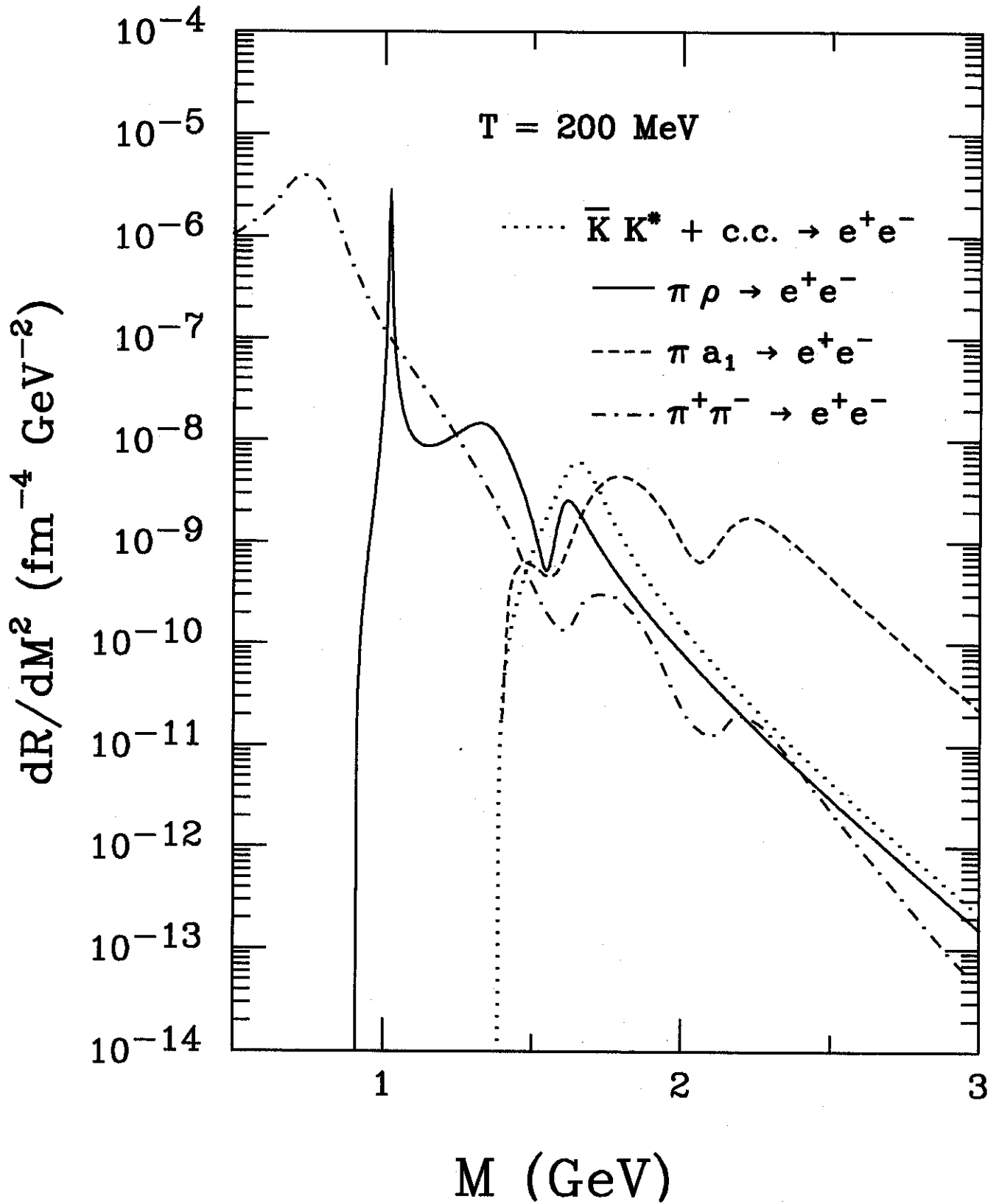


Figure 6